

1 Title: **Trends in maar crater size and shape using the global Maar Volcano Location and**
2 **Shape (MaarVLS) database**

3 Authors: Graettinger, A.H. ¹

4 Affiliation: ¹Department of Geosciences, 5110 Rockhill Road, Flarsheim Hall 420, University of
5 Missouri Kansas City, Kansas City, Missouri, 64110, USA

6 agraettinger@gmail.com

7

8 **Abstract**

9 A maar crater is the top of a much larger subsurface diatreme structure produced by
10 phreatomagmatic explosions and the size and shape of the crater reflects the growth history of
11 that structure during an eruption. Recent experimental and geophysical research has shown
12 that crater complexity can reflect subsurface complexity. Morphometry provides a means of
13 characterizing a global population of maar craters in order to establish the typical size and
14 shape of features. A global database of Quaternary maar crater planform morphometry
15 indicates that maar craters are typically not circular and frequently have compound shapes
16 resembling overlapping circles. Maar craters occur in volcanic fields that contain both small
17 volume and complex volcanoes. The global perspective provided by the database shows that
18 maars are common in many volcanic and tectonic settings producing a similar diversity of size
19 and shape within and between volcanic fields. A few exceptional populations of maars were
20 revealed by the database, highlighting directions of future research to improve our
21 understanding on the geometry and spacing of subsurface explosions that produce maars.
22 These outlying populations, such as anomalously large craters (> 3000 m), chains of maars,
23 and volcanic fields composed of mostly maar craters each represent a small portion of the
24 database, but provide opportunities to reinvestigate fundamental questions on maar formation.
25 Maar crater morphometry can be integrated with structural, hydrological studies to investigate
26 lateral migration of phreatomagmatic explosion location in the subsurface. A comprehensive

27 database of intact maar morphometry is also beneficial for the hunt for maar-diatremes on other
28 planets.

29

30 **Keywords:** maar; crater morphometry; elongation; lateral crater growth; global database

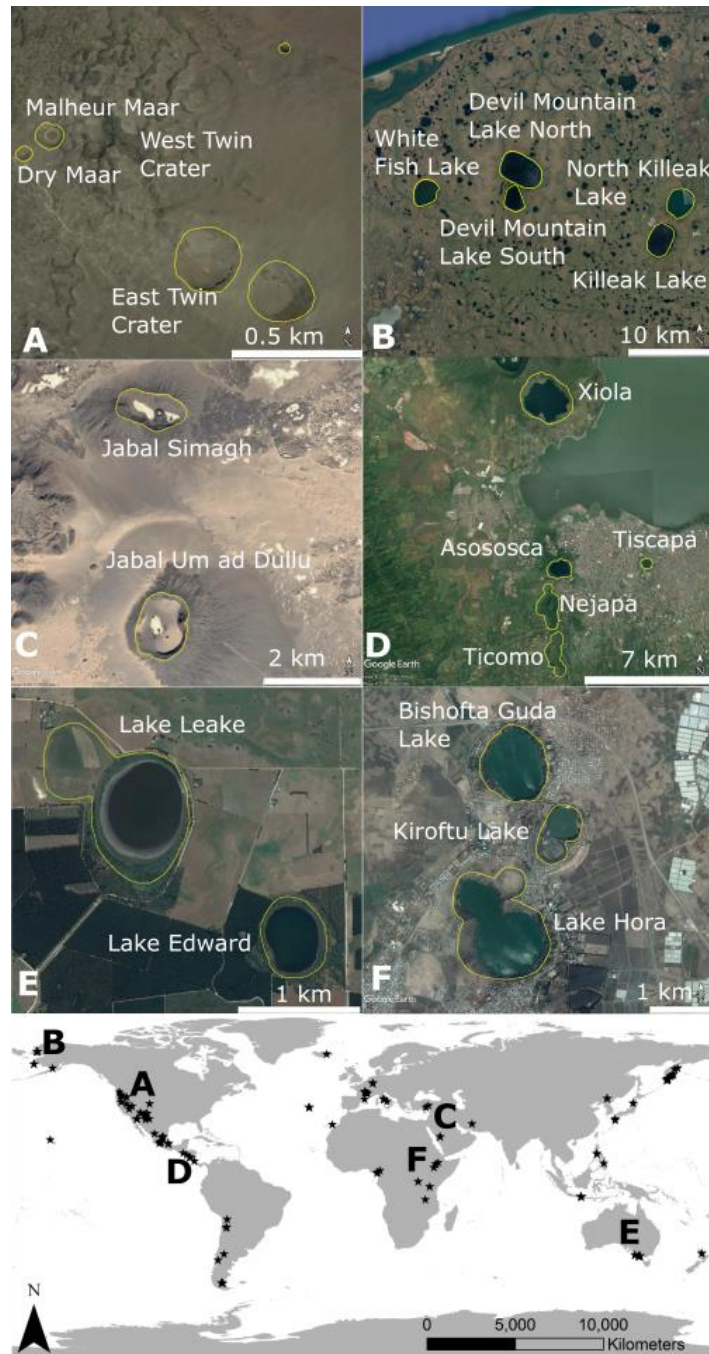
31

32 **1.0 Maar craters**

33 Phreatomagmatic explosion processes can occur in any volcanic system, but the
34 products of these processes are easiest to study at small volume volcanoes dominated by these
35 explosions. Maar craters are the end-member product of phreatomagmatic-dominated eruptions
36 and present a distinctive landform for remote morphometric analyses. Morphometry of young
37 volcanic features reflects both surface and subsurface processes of an eruption. A comparison
38 of a large population of volcanic constructs can establish the typical size and shape of craters
39 as well as any trends between the landform and local and regional influences such as volcanic
40 setting, hydrology, and topography. To recognize universal characteristics of craters formed by
41 subsurface phreatomagmatic explosions, a global database of young maar crater size and
42 shape was created: Maar Volcano Location and Shape (MaarVLS). The size of maars have
43 been previously described in a few studies, but the source data for larger datasets was
44 unavailable (Cas and Wright, 1987), the measurements are limited to a few isolated craters
45 (Nemeth et al., 2001), or were limited to highly eroded craters or diatremes (Martín-Serrano et
46 al., 2009). This database contains the data of maar sizes and shapes from multiple eruptive
47 fields from a range of volcanic settings. This study focuses on pristine morphology and thus
48 does not contain morphometric data from all known maars; however, the discussion here also
49 considers other recognized features from the literature to apply morphologic observations to our
50 understanding of maar formation. This global survey of maars enables the study of bigger
51 picture processes of these volcanoes including influences on crater growth, implication of crater
52 shape, and the diversity of features within in and between volcanic fields.

53 A maar is a volcanic crater cut into the ground surface produced by tens to hundreds of
54 discrete subsurface explosions resulting from the interaction of magma and groundwater. The
55 craters are surrounded by low angle tephra rings composed of ejecta from these explosions.
56 The dominant morphological feature of these landforms is the crater rim (Fig. 1). Maars are
57 underlain by crudely funnel-shaped structures full of pyroclastic and country rock breccias called
58 diatremes. Maars exhibit shifts in eruption style: starting with, alternating with, or ending with
59 magmatic volatile-driven activity (e.g. White and Ross, 2011). Eruptions with increasing
60 contributions from magmatic explosions form more constructional landforms such as tuff rings
61 and tuff cones that have steeper flank slopes or overlapping scoria cones. This study focuses
62 on craters produced by explosive excavation of host rock by phreatomagmatic explosions to
63 produce a crater (maar) and aims to avoid interpretations relating to the available water content.
64 As these landforms occur along a spectrum and crater infill frequently makes depth
65 measurements difficult, the database is inclusive of features with evidence of subsurface
66 excavation. To be included in the database a crater must be previously documented as a
67 phreatomagmatic construct based on field observations and meet criteria relating to age and
68 suitability for remote analysis (Table 1). Craters must be recognizable in satellite imagery
69 (visible or topographic), be Quaternary in age, and have a nearly complete to complete crater
70 rim. Consequently, some features included in the database may have been called a tuff ring or
71 cone by previous researchers because of the slope of the tephra ring deposits, but otherwise
72 meet the morphologic definition here. The use of references prevented the inclusion of any
73 known calderas, though recent work has highlighted that these features may have more in
74 common than previously recognized (Palladino et al., 2015).

75



76

77 **Figure 1** Examples of maar crater shape diversity from the MaarVLS database with yellow lines indicating
 78 the crater rim with locations of craters in the database. Locations of featured craters noted with a letter
 79 on the map. A) Diamond Crater USA including the smallest (69 m diameter) Dry Maar. B) Espenberg
 80 Craters on Seward Peninsula AK, USA are the largest craters in the database (4-5 km diameters). C) Jabal
 81 Simagh of the Harrat Kishb field in Saudi Arabia has an AR values of <0.5 . D) Nejava and Ticomo maars in
 82 Nicaragua have elongation values of <0.45 . E) Lake Leake of Newer Volcanic Province, Australia, and F)
 83 Hora Lake Bishoftu Volcanic Field, Ethiopia show off the range of isoperimetric circularities in the
 84 database. Images courtesy of Google and Digital Globe and CNES/Astrium.

Table 1: Summary of characteristics of maar volcanoes used for recognition, inclusion in the database and a revised list based on observations from the database	
Defining characteristics	Other criteria
<i>For initial recognition</i>	<i>For inclusion in database</i>
Negative landform that cuts into the ground surface	Recognized in satellite imagery including topographic datasets
Raised rim that extends away at low slope angles	Have documented field identification as a maar or fitting the description of a maar including tephra ring deposits
Rim and tephra ring composed of layers of volcaniclastic debris	Included in a publication such as peer-reviewed paper, maps or governmental information websites that can be referenced
Small <10 km in diameter	Quaternary in age
Frequently occurs in volcanic fields	Rim must be complete or nearly complete (>75%)
Additional characteristics derived from database	
Commonly elongate	
Commonly displays irregularities in curvature	
69-6000 m with most between 600-1000 m diameter	
Occur with other volcanoes either in complex or small volcano dominated fields	
Individual volcanic fields containing maars have a range of shapes and sizes	

85

86 The bulk of the explosive activity and deposits of a maar-diatreme occur in the
87 subsurface. As such, for young maars, the eruption, including depth and lateral position of
88 explosions, can only be reconstructed from the deposits that were successful ejected from the
89 crater to reach the tephra ring, and the shape of the crater. Maar craters grow through a
90 combination of explosive excavation and collapse (White and Ross, 2011; Sonder et al., 2015;
91 Graettinger et al, 2016). The crater rim is only partly a constructional feature and therefore
92 crater shape, as measured here, is less susceptible to influences of outer slope stability and
93 wind than for scoria and tuff cones (Kereszturi et al., 2012; Kervyn et al., 2012; Bemis and
94 Ferencz, 2017). These observations suggest that maar crater shape for intact crater rims retains
95 a signature of crater growth by eruptive and syn-eruptive processes.

96 Detailed studies of exhumed diatremes (Lefebvre et al., 2013; Delpit et al., 2014) and
97 geophysical investigations (Blaikie et al., 2012; Jordan et al., 2013) have revealed the
98 complexity of diatremes that can involve multiple coalesced cones of debris and reach depths of
99 up to 2 km (White and Ross, 2011). The excavation and coring of kimberlite pipes have also

100 documented overlapping diatreme structures (Kurszlaukis et al., 2009). All these observations
101 point to a complex history of magma transport and interaction with the host during these
102 eruptions. Further, the geophysical studies indicate that this subsurface complexity is linked to
103 surface complexity of maar crater shape (Jordan et al., 2013). Experimental work has
104 investigated this idea further by determining the relative distance of subsurface explosion
105 positions and the production of circular, complex, and independent craters (Valentine et al.,
106 2015a). This study aims to quantify natural maar shapes and evaluate the potential for
107 reconstructing the number and geometry of lateral explosion locations in the subsurface.

108 As with any geologic study, it is important to outline terminology and set apart descriptive
109 terms from genetic terms. The term crater here refers to the final landform, while vent is used for
110 locations where material is ejected during an eruption. Multiple vents can be located in a single
111 crater. This study uses the term compound crater to describe craters that have the appearance
112 of multiple overlapping circles, with no indication of whether that crater formed during one
113 eruptive period or several co-located eruptions separated in time. The term septum (plural
114 septa) describes a raised ridge between low points in a compound crater. The term coalesced is
115 avoided due to its inconsistent use in the past as both describing shape and reflecting a
116 polygenetic history. There are cases where field evidence indicates that a final maar crater was
117 the product of two or more eruptions separated in time that were co-located to produce a single
118 landform. Craters are documented in the database as the product of multiple eruptions only if
119 there is evidence of eruptive deposits separated by time, such as paleosols or dated eruption
120 units. This categorization here has no further implications about the longevity of the single
121 magmatic system that can be connected to the term polygenetic. In the same way, discrete
122 crater features that were produced in a single eruption (Ukinrek and Ubehebe) are included as
123 separate entries as this study focuses on shape.

124 The MaarVLS database includes manually digitized crater outlines, size, and shape
125 parameters with preliminary additional information on tectonic setting, volcanic field

126 characteristics, composition, elevation, and age. MaarVLS currently contains 240 maar craters
 127 identified in published literature as Quaternary, between -60 to 70 degrees latitude, from 65
 128 different volcanic fields (Fig. 1). The maars are predominantly mafic in composition, but five
 129 rhyolite and seven intermediate composition maars are included. The database includes
 130 historic, Holocene, and Pleistocene maars.

131 MaarVLS has room for further growth in terms of number of volcanoes and contextual
 132 information as new studies are conducted or data becomes available. The database is available
 133 on Vhub.org, an online platform for collaborative volcano research and risk mitigation, and will
 134 be updated periodically as additional submissions are collected. MaarVLS is currently a
 135 spreadsheet containing 31 categories for each crater (Table 2). All craters have name and
 136 variants, Global Volcanism Program number, latitude, longitude, country, area, perimeter, major
 137 axis, minor axis, average diameter, aspect ratio, elongation, isoperimetric circularity, volcanic
 138 field name, elevation, and references. Other categories are as complete as current literature
 139 allows and include age, composition, depth, population at 5 and 100 km distances, and whether
 140 there is evidence of multiple co-located eruptions.

Table 2: Contents of MaarVLS database.	
Contents	Details
Crater	Name, alternate name, volcano number (GVP), country
Location	Latitude and longitude of centroid using WGS-84
Shape measurements	Major axis, minor axis, average diameter (average of 2 axes), perimeter of crater, area of crater, shape type ¹
Topography ²	Depth, depth to diameter ratio, presence of septa
Context ²	Elevation, land use, tectonic setting, volcanic field type, occurrence with other maars, volcanic field name, age, evidence for multiple co-located eruptions separated in time, composition, underlying geology, population within 5 km and 100 km of volcanic field
Morphometry	Aspect ratio, elongation, circularity, depth to diameter ratio
Reference	List of references used to populate the database for a given crater
1 Polygon or shape file to indicate if the data was collected from Google Earth or using individual images in Arc GIS respectively. 2 Based on available literature, to be expanded in later versions. Elevation is measured by the level of the lake or low point of the crater.	

141

142 MaarVLS provides a global perspective on maar craters and highlights potential for
143 comparative studies between multiple volcanic fields. This study identifies the unique
144 morphometric characteristics of maars that can be used to distinguish them from other similar
145 negative landforms such as kettle and permafrost lakes, impact craters, karst features and
146 volcanic collapse pits, and can ultimately be used to identify similar volcanic features on other
147 planets, such as Mars (Graettinger, 2016).

148 **2.0 Methods**

149 Maar craters were selected from existing literature in areas where satellite imagery was
150 most readily available. Literature here includes peer-reviewed articles, edited books on volcanic
151 regions, the Global Volcanism Database (Global Volcanism Program), field trip guides, city and
152 federal government informational websites, and USGS or US National Parks Service
153 publications and maps. The references for individual craters are included in the database and a
154 comprehensive reference list accompanies the database (Supplemental information). Craters
155 were initially located using published coordinates and maps, and then added to a Google Earth
156 .kml file and evaluated for morphometric analysis. Google Earth uses a cylindrical projection
157 that has significant warping at the poles. This first version of the database only includes craters
158 above 60 degrees latitude when alternative datasets such as Advanced Spaceborne Thermal
159 Emission and Reflection Radiometer (ASTER) imagery were already available in the author's
160 collection. Future versions of the database will take advantage of publicly available ASTER
161 imagery and other open datasets to include a larger population of maar craters at high latitudes.
162 All craters are Quaternary in age and have complete, or near complete (>75%), rims with limited
163 incision by erosion (Table 1). Craters that have interacted with scoria cones or lava flows were
164 generally avoided, unless the 75% unobstructed crater rim criterion was satisfied. Compound
165 craters with > 3 separated basins are not included in the first version of the database due to the
166 high level of interpretation required for digitization (i.e. Katwe Volcanic Field, Uganda; Murray

167 and Guest, 1970). Modification by human activity is common for many of the volcanic fields
168 studied. When human activity made an obvious impact on the crater rim (i.e. quarrying), the
169 crater was not included in the database.

170 Craters were outlined manually from visible Google Earth imagery, ASTER images and digital
171 elevation models to produce polygons encompassing the crater along the rim. Crater outlines
172 were completed by four individuals and evaluated by one researcher for consistency. Polygons
173 of crater outlines were used to determine area, perimeter, and length of major and minor axes.
174 An average of the two axes is used as average diameter in this study. Shape parameters were
175 derived for each crater from these measurements. Shape parameters used in this study
176 describe the two-dimensional shape of the outline of the crater from the digitized polygon.
177 These include dimensionless ratios: aspect ratio, elongation, and isoperimetric circularity.
178 Aspect ratio (AR) is defined as the ratio of a crater's diameters:

$$179 \quad AR = \frac{D_{minor}}{D_{major}} \quad (1)$$

180 where D_{minor} is the length of the crater's minor axis and D_{major} is the length of the crater's
181 major axis. Here the minor axis is measured as the axis perpendicular to the major axis running
182 through the center point. An aspect ratio of 1 represents an equant shape around the center
183 point; as the disparity between the two axes increases, the aspect ratio decreases away from 1.

184 Elongation (EL) is defined:

$$185 \quad EL = \frac{A}{\pi\left(\frac{D_{major}}{2}\right)^2} \quad (2)$$

186 where A is the area encompassed by the crater rim as defined by the digitized polygon.
187 Elongation compares the area of a circle with the diameter of the major axis to the maar area. A
188 circle has Elongation equal to 1 and more elongate shapes have smaller values. Elongation

189 differs from Aspect Ratio as it better describes asymmetrical shapes, in fact, for ellipses the two
190 values will be the same.

191 Isoperimetric Circularity (*IC*) is defined as the area of a crater polygon divided by the
192 area of a circle with the same perimeter.

$$193 \quad IC = \frac{4\pi A}{P^2} \quad (3)$$

194 where *A* is the area encompassed by the crater rim and *P* is the perimeter of that same polygon.
195 Isoperimetric Circularity is a measure of the variation in curvature of the outline of a shape. A
196 shape with a single constant angle of curvature, like a circle, has an Isoperimetric Circularity of
197 1 and shapes where the angle of curvature varies will have Isoperimetric Circularity <1.

198 Depth measurements for craters were collected from the literature, using topographic
199 data such as the Earth Point topo map of the US, published topographic maps of field areas,
200 and estimates in publications or from local governments (city, state/province) or national parks.
201 These values are only as accurate as their source material and therefore have an uncertainty of
202 at least 10 m. Due to the presence of lakes, inconsistent reporting, post-eruption modification by
203 erosion, human or volcanic activity, and low resolution data, maximum depth measurements
204 reported are minimums. Where the measurement reflects only the surrounding rim, or only lake
205 depth, a notation is included in the database. Depth to diameter ratio (*d/D*) was calculated for
206 craters when possible using the available values for depth by the major axis and is
207 consequently a minimum value. Elevation is recorded at the base of the tephra ring or the
208 surface of lake in the maar as available, and other available published estimates. Due to limited
209 data availability, some volcanic fields have single elevation reported across the field. No values
210 are expected to be off by more than 200 m. Although not useful for in-field evaluations, these
211 values are sufficient for preliminary evaluation and will be an area of improvement in later
212 versions of the database. This study addresses quantitative size and shape parameters, latitude
213 and longitude, elevation, composition, and when possible, age of maar craters. Volcanic fields

214 that host maars are discussed based on the maars included in the database (with well-
215 preserved morphologies), and not total population.

216

217 **3.0 Results**

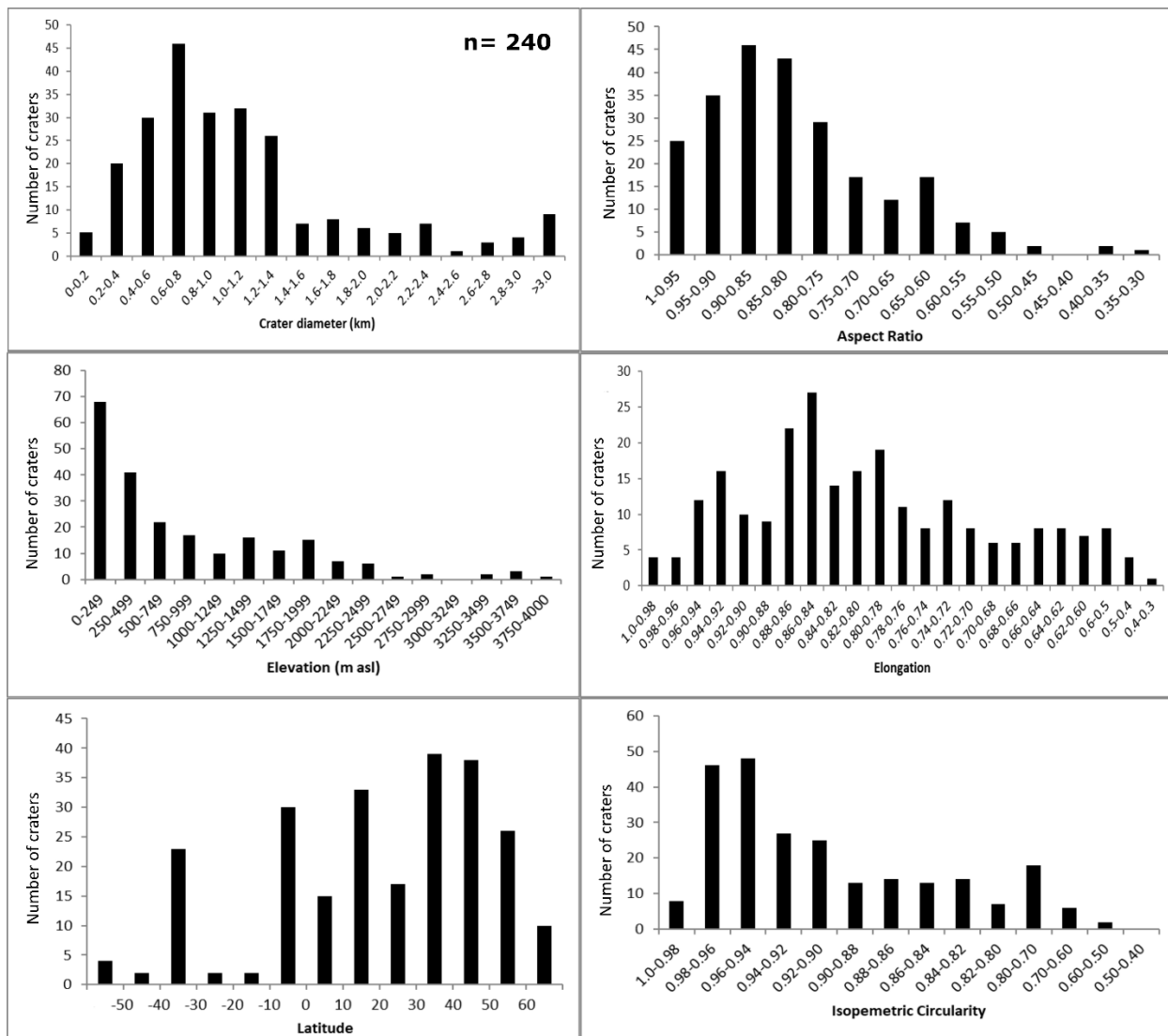
218 *3.1 Size and Shape*

219 Mean crater diameters, the average of the two major axes, in MaarVLS are 69-5000 m.
220 Major axis measurements reach up to 6100 m, and minor axes measurements reach 4300 m.
221 The smallest maar, the 69 m mean diameter Dry Maar, occurs in the Diamond Craters field in
222 Oregon, USA (Wood and Kienle 1990; Fig. 1a). The largest maar, the 5013 m mean diameter
223 Devil Mountain Lake North, occurs in the Espenberg volcanic field in Alaska, USA (Beget et al.
224 1996; Fig. 1b). Most maar craters have diameters 600-800 m (Fig. 2); 75% of the average crater
225 diameters are <1295 m. Crater areas average 1.5 km², with perimeters of 0.2-16 km. The
226 smallest maars (<200 m, <3% of database) occur in close proximity (<600 m) to other maar
227 craters including the Ukinrek West crater (Self, 1980) and Crater Z at Ubehebe (Fierstein and
228 Hildreth, 2017). In several cases these small craters are interpreted to be part of the same
229 eruptive sequence as the adjacent craters (Self, 1980; Fierstein and Hildreth, 2017). Very large
230 craters (>3000 m diameter and area >7 km²) represent only 4% of the maar population.

231 Available values for maar depths range 5-400 m with an average depth to diameter ratio
232 of 0.10. However, depth estimates are poorly constrained with error estimates of ~20 m due to
233 the presence of lakes and abundance of sedimentary infill. For the 113 craters in the database
234 with both depth and age data, there is no apparent trend of depth with age (Fig. 3). As depth is
235 susceptible to post-eruption infill (Pirrung et al., 2008), subsidence (White and Ross, 2011), and
236 human modification, preserved depth is not reflective of eruption history and therefore not
237 discussed further in this analysis. Only 7% of the craters in the database have septa separating
238 the circular elements of the crater shape (e.g. Ticomo, Nicaragua; Figure 1; Avellan et al.,

239 2012). In craters without septa the lowest point is frequently off center and some compound
 240 craters have a stepped topography (e.g. Kiroftu Lake, Ethiopia; Gasparon, 1993).

241

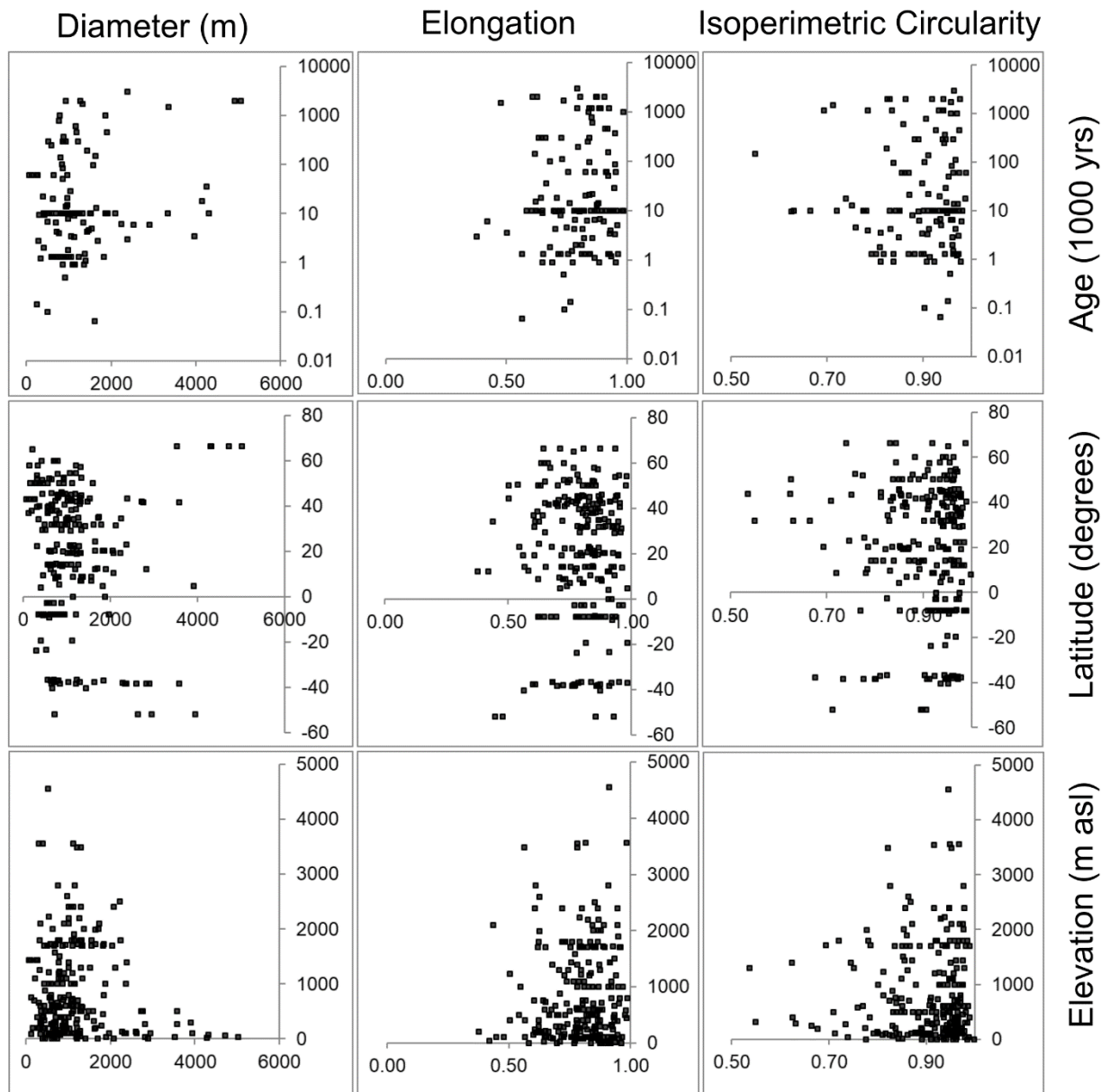


242 **Figure 2** Histograms of craters in MaarVLS version 1 database including size, distribution and shape. The
 243 total number of crater is 240.
 244

245

246 Aspect ratio is a measure of the disparity between the major and minor axis (Equation
 247 1). Maar craters have an average Aspect Ratio of 0.81 with most values between 0.80-0.95
 248 (Fig. 2). Less than 11% of maars have an Aspect Ratio >0.95 reflecting an equant shape.

249 Extreme low values of Aspect Ratio (0.3-0.5) describe only 2% of the database (e.g. Jabal
250 Simagh Saudi Arabia; Fig. 1c).



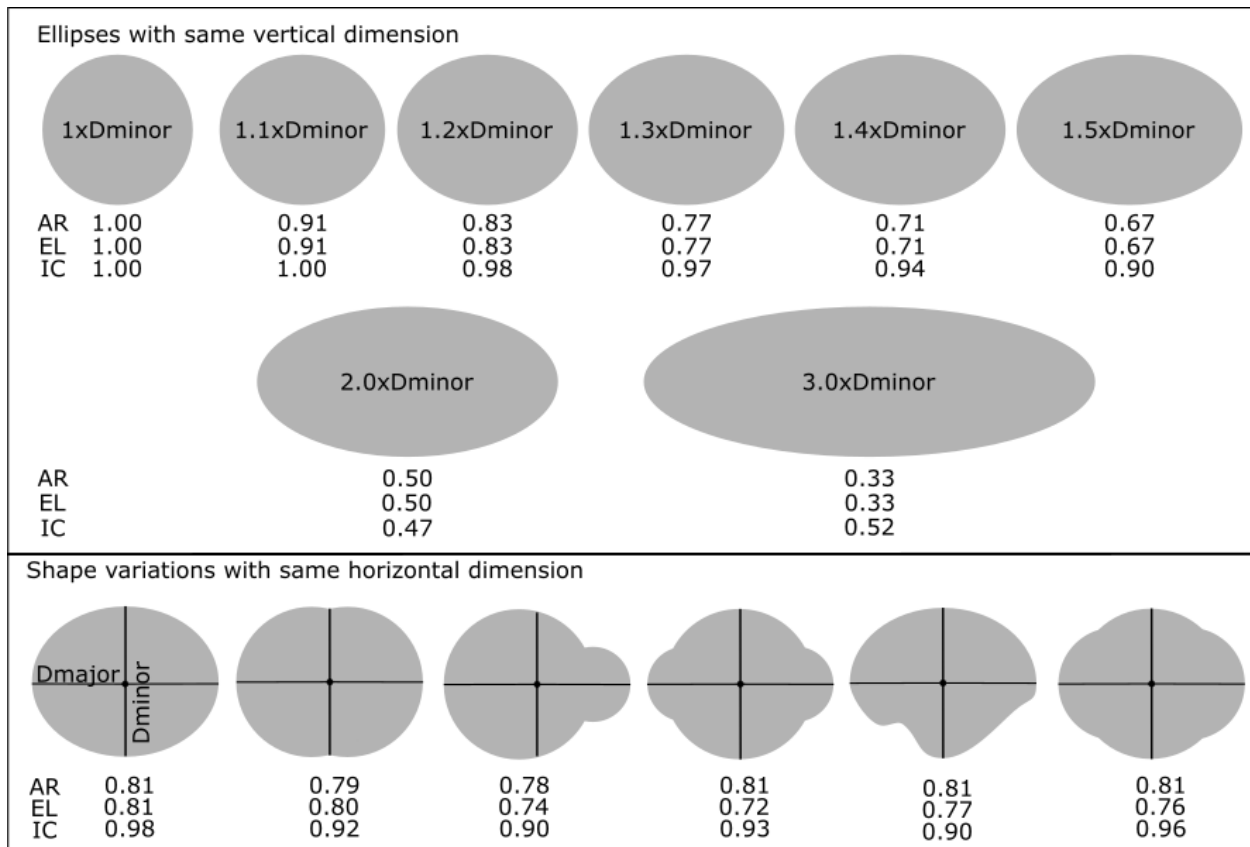
251
252 **Figure 3** MaarVLS crater shape and size parameters relative to distribution (elevation and latitude) and
253 age. The diameter is the crater average. Elongation of a circle is 1.0 and more elongate shapes >1.0.
254 Isoperimetric circularity of a circle is 1.0 and less circular shapes are <1.0. There are no distinct trends
255 between shape and size with age. Small craters occur at all latitudes and elevations but exceptionally
256 large craters are found predominantly at high latitudes and low elevations.

257

258 Elongation compares the area of the maar to the area of a circle with the diameter of the
259 major axis (Equation 2). The craters in the database have a wide range of Elongation, averaging
260 0.80 with a standard deviation of 0.12 and most values between 0.88-0.84 (Fig. 2). In MaarVLS
261 85% of craters have Elongation values less than 0.92. Extreme values of Elongation (<0.50)
262 reflect only 5% of the database (e.g. Nejapa Maar, Nicaragua; Fig. 1d).

263 Isoperimetric Circularity is a measure of the variation in curvature of the outline of a
264 shape with values 0-1 with 1 being a circle. (Equation 3). Maar craters in the database have a
265 limited Isoperimetric Circularity, with average values of 0.9 and standard deviation of 0.08. Most
266 (65%) craters have an Isoperimetric Circularity 0.9-1 (e.g. Lake Leake, Australia; Fig. 1e; Boyce,
267 2013) with only 9% of craters having a value below 0.80 (e.g. Hora Lake, Ethiopia; Gasparon
268 1993; Fig. 1f). Maar craters with Isoperimetric circularity values <0.9 display a compound shape,
269 similar to multiple overlapping circles (Fig. 4) resulting in a few larger scale variations in
270 curvature. There is no apparent trend with size for any of the shape parameters (Fig. 3). There
271 is not a diagnostic crater shape related to craters produced by multiple co-located eruptions or
272 long-lived polygenetic eruptions. This relationship will need to be reevaluated as more dates
273 become available for these volcanic systems.

274 These shape values can be compared with ellipses that vary by the relationship between
275 the major and minor axis (Fig. 4). The average Aspect Ratio and Elongation of maars in the
276 database can be reproduced by an ellipse with a major diameter >1.2 times that of the minor
277 diameter. These ellipses, however, both have greater Isoperimetric circularity values than the
278 average maar crater. Additionally, most maars do not have equivalent AR and EL values the
279 way that ellipses do. Natural maars commonly have compound shapes resembling overlapping
280 circles or embayed ellipses. A series of simplified shapes with AR, EL and IC values close to the
281 database average illustrates how the shape values respond to symmetry and curvature
282 variations (Fig. 4) common in the database.



283
 284 **Figure 4** Idealized shapes that illustrate how shape parameters vary with shape complexity. Ellipses
 285 where the maximum diameter increases relative to the secondary diameter (D_{minor}) show how aspect
 286 ratio and elongation decrease drastically with exaggerated ellipses. AR and EL values <0.5 are considered
 287 extreme and represent less than 5% of the database. The AR values from the database correspond to
 288 ellipses with major diameters 1.1-1.3 times that of the minor diameter, but the isoperimetric values
 289 require changes in curvature of the shape as exemplified by the lower shapes.

290
 291 **3.2 Distribution**

292 Maar craters occur in 1) monogenetic fields with similar sized volcanic features such as
 293 scoria cones (56% of database), 2) in complex volcanic fields containing small volcanic vents
 294 alongside, on, or, in larger structures such as stratovolcanoes and calderas (42%), and 3) in
 295 rare cases, in isolation. Over 96% of craters in the database occur in fields with other maars,
 296 where 71% of craters occurred in fields with more than five maars. While roughly half of the
 297 maars in the database occur in intraplate volcanic settings, they are also found in back arc

298 basins along subduction zones, continental rifts, on ocean islands above hot spots, and less
299 commonly in convergent or transpressional environments.

300 Maars in the database occur at sea level to elevations as high as 4000 m above sea
301 level (asl). At higher elevations the number of documented maars decreases, with most (90%)
302 below 2000 m asl (Fig. 3). Maars in the database cover a range of latitudes, but do not have
303 even distribution across all latitudes (Fig. 2). Maars above 200 m all occur between -30 and 40
304 North latitude. A comparison of crater diameter with distribution reveals that small craters
305 (<1000 m) occur globally at all elevations (Fig. 3), however, all exceptionally large maar craters
306 (diameter >3000 m, area >7 km²) occur at elevations below 500 m asl. Crater shapes do not
307 present a clear trend with latitude, but isoperimetric circularity does increase (craters are more
308 circular) with increasing elevation (Fig. 3).

309 3.3 Fields

310 Quaternary volcanic fields with maar volcanoes contain anywhere from one to tens of
311 maar craters. In MaarVLS several fields are currently represented by only a sample of maars
312 due to limitations in available imagery, and the complete crater rim criterion. For volcanic fields
313 with five or more included maar craters, the size variability within individual volcanic fields is
314 high, but lower than the database as a whole (measured in meters; total stdev=861, for fields
315 with maars stdev=395; Table 3). Within a volcanic field, craters will typically fit between a
316 minimum and maximum crater diameter ratio of 0.36, meaning that the largest crater is less
317 than twice the diameter of the smallest crater. The shapes of craters within these volcanic fields
318 have similar average shape parameters, but narrower ranges than the overall database (Table
319 3).

320

321

Table 3: Comparison of maars globally to trends by volcanic fields containing maars.

	Average diameter (m)	Aspect Ratio	Elongation	Isoperimetric circularity	n	Diameter range (m)	Min dia/ Max dia ratio
MaarVLS	1122+/- 833	0.81+/- 0.13	0.80+/-0.12	0.90+/-0.08	240	4945	0.01
Mode	603	0.84	0.62	0.93			
50 percentile	905	0.83	0.82	0.93	240		
Fields containing 5 or more maars	1179+/- 395	0.81+/- 0.05	0.79+/-0.05	0.90+/-0.04	5*	1148	0.36
Mode	600-800	0.75-0.85	0.79-0.80	0.85-0.95	2-19**		

Values are averages +/- one standard deviation or represent a range.
 Volcanic fields used for this analysis: Auckland Volcanic Field (NZ), Bishoftu Volcanic Field (Ethiopia), Chaine des Puys (France), Diamond Craters (USA), Eifel Volcanic Field (Germany), Lake Natron-Engaruka field (Tanzania), Lamongan (Indonesia), Long Gang (China), Newberry volcanic region (USA), Newer Volcanic Province (Australia), Pinacate Volcanic Field (Mexico), Qal' eh Hasan Ali (Iran), San Pablo Volcanic Field (Philippines), Serdán Oriental (Mexico), Espenberg Volcanic Field (USA).
 *Average value for all volcanic fields in the database containing more than one maar.
 ** Range of values for the number of maars in fields with more than one maar in database.

322

323 The database also provides an opportunity to investigate the distribution of maar craters
 324 relative to population centers (Table 4). Based on population data 2013 as recorded by GVP six
 325 volcanic fields with more than 5 Quaternary maars occur within 5 km of >100,000 people. The
 326 Auckland Volcanic Field in New Zealand, Nejapa-Miraflores Field in Nicaragua, and San Pablo
 327 City Volcanic Field in the Philippines are within 5 kilometers of more than a million people.
 328 These population values should be considered conservative estimates as urban populations are
 329 growing globally and areas like Addis Ababa close to the Bishoftu Volcanic Field in Ethiopia,
 330 have large undocumented populations not reflected in these estimates.

331 3.4 Age

332 Age constraints are available for 53% of the database (n=127), and only half of those
 333 are isotopic techniques applied to the maar deposits, stratigraphically bounding units or historic
 334 observations with the remainder being based on morphology and comparisons with features in

335 the same volcanic field. However, as individual volcanic fields containing multiple maar craters
 336 (e.g. West Eifel Volcanic Field, Zolitschka et al., 1995) are well dated, the preliminary trends
 337 between crater size, shape and distribution with age were evaluated. There is no apparent
 338 correlation between maar crater age with latitude, elevation, diameter, elongation or
 339 isoperimetric circularity (Fig. 3).

Table 4: Volcanic fields containing multiple maar volcanoes occur near large population centers around the world. Populations within 5 km of maars and maar fields are at risk of primary eruption hazards such as ballistic fall and pyroclastic density currents.

Name	N ^a	# of vents ^b	Min Diameter (m)	Max Diameter (m)	Population within 5 km ^c
Auckland, New Zealand	7	53	333	1229	1,500,000
Bishoftu, Ethiopia	6	>20	766	1556	300,000
Chaîne des Puys, France	9	141	440	1336	300,000
Eifel, Germany	11	224	158	1593	90,000
Lake Natron-Engaruka, Tanzania	5	200	550	871	low
Lamongan, Indonesia	19	90	349	1211	>5,000
Long Gang, China	5	>150	742	1125	30,000
Nejapa-Miraflores, Nicaragua	5	>10	622	2824	2,200,000
Newberry, USA	6		789	2379	<100
Newer Volcanic Province, Australia	13	416	640	3582	<600,000
Pinacante, Mexico	9	>400	650	1782	<100
Qal'eh Hassan Ali, Iran	5	5	438	1333	5,000
San Pablo, Philippines	12	tens	564	1268	1,300,000
Seridán Oriental, Mexico	8	tens	1010	2218	90,000
Seward, USA	5	5	3532	5013	Low
Kamchatka, Russia	12	100's	312	1339	Low

^a number of maars in field included in the MaarVLS database, represents a minimum value for maar population within the volcanic field.
^b number of vents (all types) in the field from GVP, LeCorvec 2013; Mattson and Tripoli 2011; Carn 2000; Boyce 2013; Gutman 2002; Milton 1977.
^c Population data from GVP 2013 and are rounded down to the nearest 5,000 to provide relative numbers rather than precise population values. Population values for Nejapa-Miraflores updated to reflect 2015 population of Managua.

340

341

342

343 **3.5 Composition**

344 Compositional data are available for 60% of the database (n=146). Most maars in
 345 MaarVLS were formed by mafic magmas, with high alkali contents common. Five confirmed
 346 rhyolitic maars and seven intermediate maars are included in this first version of the database.
 347 The rhyolitic maars are all larger than 1000 m in diameter, but are not distinctively larger than
 348 mafic maars as a population (Table 5). Intermediate magmas form maar craters 360-1400 m
 349 across and fit within the scatter of mafic maar sizes. The shape of intermediate and rhyolite
 350 maars is typically more circular and less elongate than mafic maars, but not enough to be
 351 diagnostic. The largest craters (>3000 m) are limited to mafic magma compositions. Therefore,
 352 based on this population, composition cannot be determined solely from crater size or shape.

Table 5: Comparison of size and shape trends for maars with known magma compositions.

	Average diameter (m)	Aspect Ratio	Elongation	Isoperimetric Circularity	n	Diameter range (m)	Min dia/ Max dia ratio
Mafic	1236 +/- 1023	0.80 +/- 0.14	0.79 +/- 0.13	0.90 +/- 0.08	134	4945	0.01
Intermediate	760 +/- 516	0.86 +/- 0.08	0.87 +/- 0.07	0.90 +/- 0.05	7	1479	0.20
Rhyolite	2017 +/- 923	0.91 +/- 0.08	0.88 +/- 0.08	0.96 +/- 0.03	5	1814	0.36

Values are averages +/- one standard deviation or represent a range.

353

354 **4.0 Discussion**

355 The MaarVLS database enables several generalizations about maar crater size and
 356 planform shape that were previously not possible due to the absence of a global dataset. Maar
 357 craters are typically elongate, but not simple ellipses, having large-scale variations in curvature
 358 that frequently resemble overlapping circles. Although compound shapes are common, septa
 359 separating topographic lows are rare (or rarely preserved), and the organization of the
 360 overlapping circles is variable across maars and volcanic fields with maars (Fig. 1). A few
 361 anomalous populations of maar size (exceptionally large) and morphology (crater chains) stand
 362 out against the main database characteristics. The database also highlights that while maars

363 typically represent a fraction of the volcanic constructs within a volcanic field there are a few
364 notable exceptions with abundant maars. Further, the maars studied occur in a wide range of
365 volcanic field types and tectonic settings reinforcing that while the conditions that form maar
366 volcanoes are specific, they are not limited to only one environment. Further, the global
367 distribution of maars highlights the proximity of numerous maar fields to major population
368 centers. In order to evaluate the potential for interpreting subsurface maar forming processes,
369 namely explosion location and number, from crater shape it is necessary to evaluate post-
370 eruption modification, the completeness of the sample population, and the exceptional maar
371 populations mentioned above.

372 *4.1 Role of post-eruption modification*

373 Investigations of crater modification from the 1977 eruption of Ukinrek in Alaska revealed
374 a rapid increase in the major and minor axes of the crater and infill of the crater floor initially
375 after the eruption and stabilization with time (Pirrung et al., 2008). The shape of the crater
376 however, as measured by aspect ratio, was maintained. This suggests that absolute crater
377 diameters, depth, and internal slopes are susceptible to modification by erosion, but crater
378 shape is more stable over time. As the inclusion criterion for MaarVLS excluded maar craters
379 such as Kilbourne Hole, New Mexico, and Fort Rock, Oregon where the crater rim was
380 interrupted or missing, the shapes within the database are assumed to represent post-eruptive
381 shapes. Furthermore, comparison of Aspect Ratio, Elongation, and Isoperimetric Circularity for
382 those maars in the MaarVLS database with age indicates that there is no trend in crater shape
383 with age for Quaternary maars (Fig. 3).

384 Unlike scoria cones, which are constructional features with steep slopes, maar craters
385 have low angle tephra rings that extend away from the crater with the main structure cut into the
386 ground surface. When maars are erupted on complex topography this tephra ring will roughly
387 drape the surrounding topography (e.g. Dotsero, Leat et al., 1989; Bea's Crater, Amin and
388 Valentine, 2017). The crater is the result of excavation and collapse with limited deposits

389 escaping the crater to form the low angle tephra ring (Graettinger et al. 2016). The shape of the
390 crater is therefore less susceptible of the influence of outer slope stability and wind than for
391 scoria and tuff cones (Kereszturi et al., 2012; Kervyn et al., 2012). The low slope angle of the
392 tephra rings enables agricultural activities with less earth works than scoria cones or lava flows,
393 and consequently many roads and farms merely mantle the tephra ring deposits preserving
394 crater rim morphology. Based on these observations, for maars included in the database it is
395 reasonable to assume the crater shape, and to a lesser degree crater size, is dominated by a
396 signature of crater growth by eruptive and syn-eruptive processes.

397 *4.2 Completeness of coverage*

398 MaarVLS contains craters from a range of latitudes, with fewer craters at latitudes
399 greater than 60 degrees. High latitudes in both hemispheres are under-sampled as additional
400 imagery is required (due to warping of projections at the poles in WGS84 used in Google Earth)
401 and will be used to produce future versions of the database. The southern hemisphere is
402 represented by 64 craters, with limited craters from -10 and -20 degrees (Fig. 2). As the
403 southern hemisphere contains ~30% of the continental crust on Earth, the database has a
404 roughly proportionate distribution of maar craters between the hemispheres. Maar craters are
405 observed at a wide range of elevations (0-3500 m asl), but 60% of maars are at elevations of
406 1000 m or less, with half of that being at elevations below 250 m. As 75% of elevations above
407 sea level on Earth are less than 1000 m (Eakins and Sharman, 2012) the low abundance of
408 maars at high elevation is to be expected (Fig. 2). The number of craters included in the
409 database and the large range of elevations and latitudes on Earth provides a sufficiently diverse
410 population to establish what is typical of maar crater size and shape (Section 3.1) to recognize
411 any exceptional populations of maars on Earth (Fig. 2-3).

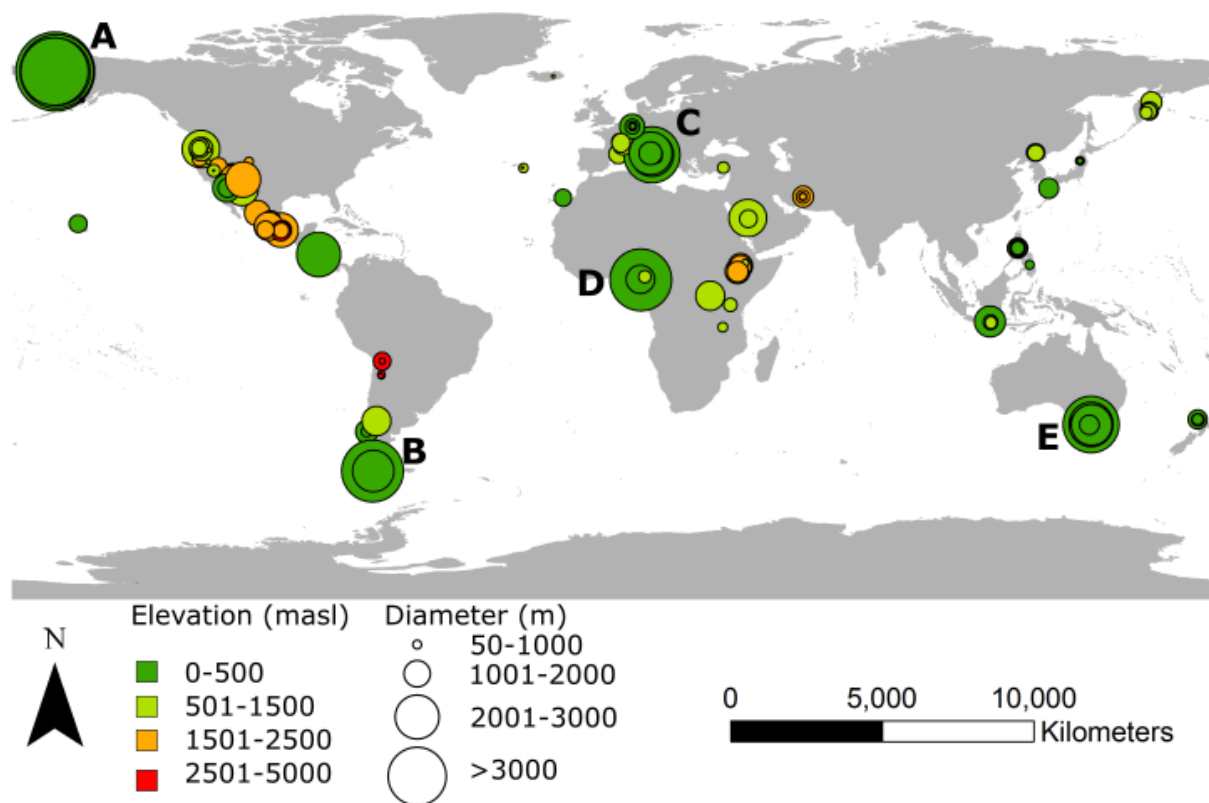
412 *4.3 Unique populations*

413 *Very large craters*

414 Of the shape parameters evaluated, diameter (Fig. 2) and area are the only parameters
415 to highlight a distinct outlying population. Very large maars occur in six volcanic fields that are
416 globally distributed, but all occur at low elevations (Fig. 5). The Espenberg maars (Beget et al.,
417 1996) in Alaska, USA, and Pali Aike maars in Argentina (Ross et al., 2011) both include multiple
418 craters >3000 m in diameter that are thought to have erupted through permafrost based on field
419 observations. Field studies have indicated that soft host rock may lead to larger crater diameters
420 (Auer et al., 2007), however the size of these craters far exceeds the database norm and the
421 size of other maars formed in unconsolidated sediment. These large high latitude maars
422 suggest that the distribution and physical state of water in the host rock may also be significant
423 to crater size and shape. In particular, the nature of the host rock influences the availability and
424 transport of water within a diatreme required for phreatomagmatic explosions. Because the
425 extent of permafrost during past glaciations is not well constrained and maar age dates are still
426 sparse there may be additional craters (of any size) that formed in a glacial or periglacial
427 environment. The role of ground ice in the formation of maars is an important area of exploration
428 on Earth and on Mars.

429 The majority of the remaining >3000 m maars occur in complex volcanic fields including
430 Colli Albani in Italy and Kumba in Cameroon, and show evidence of multiple eruption deposits
431 separated by paleosols (Sottili et al., 2009; Chako Tchambe et al., 2015). All maars in the
432 database with evidence of multiple co-located eruptions are > 1000 m in diameter (Nemeth and
433 Kereszturi, 2015; Jordan et al., 2013; van Otterloo et al., 2013; Isaia et al., 2015; Valentine et
434 al., 2015b), but not all large craters show evidence for multiple eruptive episodes (e.g.
435 Espenberg maars, Beget et al., 1996). Those craters that have experienced multiple co-located
436 eruptions occur in both continental rift settings like the Kumba field and in back arc basins such
437 as the Nejapa maar in Nicaragua (Avellan et al., 2012). Maars produced by co-located eruptions
438 occur with other small volume volcanoes in the Newer Volcanic Province, Australia (van

439 Otterloo et al., 2013), and in conjunction with long-lived composite volcanoes like the Sabatini
 440 District in Italy (Valentine et al., 2015b). The Newer Volcanic Province hosts several large
 441 maars, some exceeding 3000 m in diameter, however additional work is required to determine if
 442 they were all the product of multiple co-located eruptions. The relationship between
 443 exceptionally large maar craters and their eruptive hazards including duration, potential for
 444 repeat eruptions and scope of eruption, warrants further exploration in these and other volcanic
 445 fields.



446
 447 **Figure 5** Crater size (average diameter) and elevation plotted geographically with one symbol per maar,
 448 but significant overlap occurs due to the size of the map. Labeled fields host very large maar craters
 449 (>3000 m diameter) A) Espenberg maars, B) Pali Aike Volcanic Field, C) Colli Albani Volcanic Region, D)
 450 Kumba Volcanic Field, E) Newer Volcanic Province. Large maars all occur below 500 masl.

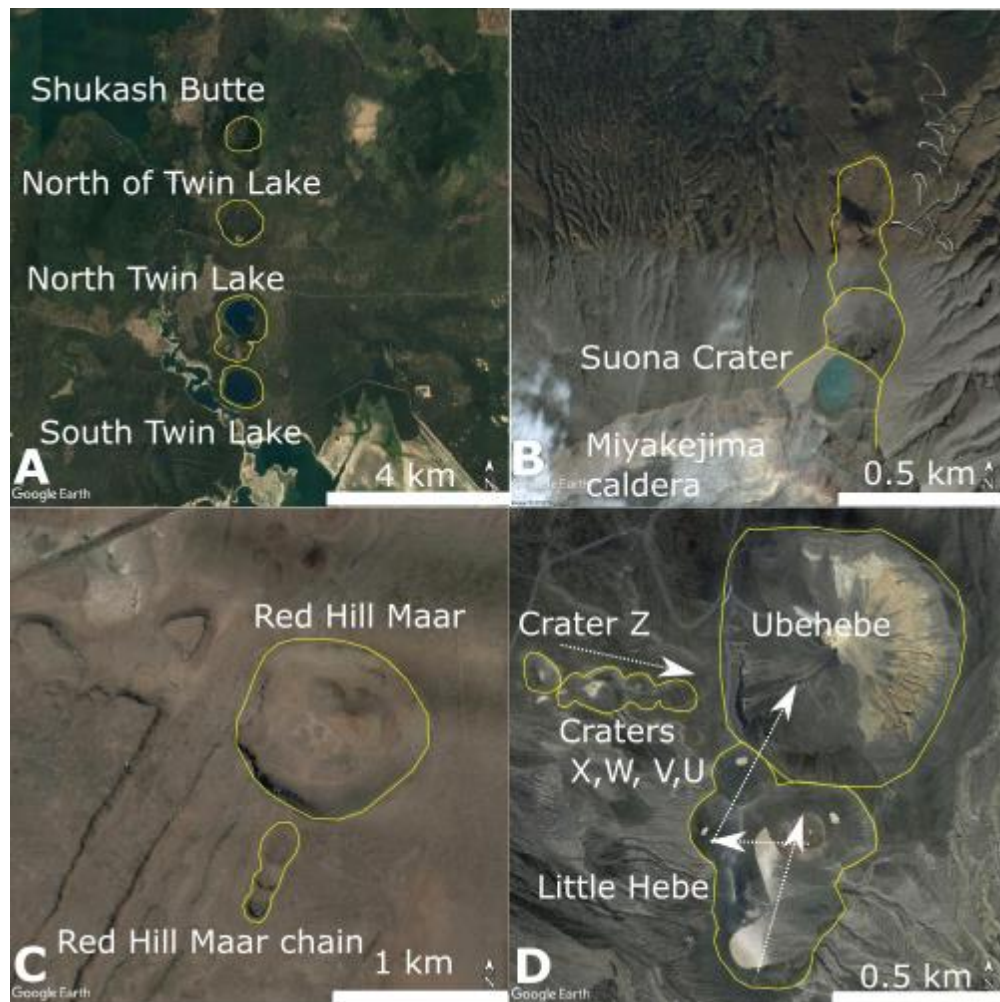
451

452

453 *Chains of craters*

454 An additional subgroup of maar craters resemble chains of closely spaced or connected
455 craters with associated extreme values of Elongation and Aspect Ratio. The Asososca, Nejapa,
456 and Ticomo maars in Nicaragua south of Lake Managua, occur along a linear trend that could
457 be extended to include the Xiola maar to the north (Fig. 1d). Within this set of closely spaced
458 aligned craters, the Nejapa and Ticomo maars are both composed of a chain of several
459 connected depressions (Avellan et al., 2012). The Twin Lakes cluster in Oregon, USA occurs as
460 a closely spaced set of four aligned craters parallel to the Cascade Volcanic arc, where the
461 compound North Twin Lake is composed of two connected depressions and sits <100 m north
462 of the South Twin Lake crater rim (Fig. 6a). Although not suitable for the database because of
463 truncation by the Miyakejima caldera, Suona crater Japan is one of several overlapping maar
464 craters, separated by septa that form a chain (Fig. 6b). There are also much smaller diameter
465 crater chains associated with average sized maars, such as Ubehebe Crater in California USA
466 that has the prominent ~800 m Ubehebe crater, the Little Hebe complex of overlapping
467 phreatomagmatic and magmatic vents to the south, plus a much smaller related chain of
468 explosively excavated craters to the west (Fierstein and Hildreth, 2017; Fig. 6d). This resembles
469 the Red Hill maar that has a disconnected chain of three craters to the south (Chamberlin et al.,
470 1994; Fig. 6c). The Nejapa, Twin Lake, and Suona craters all occur in complex volcanic fields,
471 while the smaller chains at Ubehebe and Red crater occur in relative isolation. Although
472 temporal data is not available for all of these examples, the Nejapa-Miraflores maars and
473 Ubehebe indicate that the craters were not formed simultaneously along a single fissure, and
474 were the result of lateral migration of explosion locations.. Subsurface explosions that occur in
475 different lateral positions but have overlapping explosion footprints produce circular to
476 compound shapes (Valentine et al., 2015a) and are likely to have complex tephra rings. When
477 explosions are spaced further apart, they can form a linked chain of craters (Valentine et al.,

478 2015a). Additionally, the preservation of discrete craters in a chain suggests there has been
479 little to no syn-eruptive collapse of the crater rim, preserving a more complete record of ejecta.



480
481 **Figure 6** Examples of closely spaced or chains of maar craters mentioned in the text, not exhaustive of
482 the database. A) Twin Lakes Oregon, USA; B) Suona crater (not included in database) and associated
483 crater chain on Miyakejima volcano Japan; C) Red Hill Maar and chain, US; D) Ubehebe Crater, USA.
484 White arrows represent general direction of vent locations from Fierstein and Hildreth (2017) where the
485 final state of the eruption was from the main Ubehebe Crater. Images from Google Earth.
486

487 *Maar-dominated volcanic fields*

488 While maars are a common in both complex and small volume volcano fields, they
489 typically make up a small percentage of the volcanic landforms in a given field. In large fields of

490 small volcanoes (monogenetic fields) maars typically represent a few percent of the total vent
491 population, for example the Newer Volcanic Province has 10% phreatomagmatic constructs of
492 416 with only 21 being strictly maars (Boyce, 2013) and the Pinacate Field in Mexico has 2%
493 phreatomagmatic constructs out of >400 vents (Gutmann, 2002). In complex volcanic fields,
494 maars can represent a larger percentage of the vents, but only a small volume of erupted
495 material. In the Lamongan Volcanic field in Indonesia maars make up 30% of the preserved
496 vents, but they are scattered around the base of a 1631 m tall Lamongan stratovolcano (Carn,
497 2000). The San Pablo Volcanic field contains at least 12 maars and sits in the Macolod Corridor
498 in the Philippines nestled between Taal Caldera and several stratovolcanoes as well as dozens
499 of scoria cones (Ku et al., 2009). There are, however, a few volcanic fields that are dominated
500 by, or wholly composed of maar craters. The craters within these volcanic fields are frequently
501 remote and poorly studied, and thus not all have representative craters in of the MaarVLS
502 database. Along the East African Rift Katwe-Kikorongo near Lake Edward and Kyatwa/Ndale in
503 Uganda, as well as the Bilate River Field in Ethiopia are composed almost entirely of maar
504 craters. Other fields in the rift like Fort Portal and Bunyaruguru in Uganda are composed of
505 maars, tuff rings, and lava flows (Kampunzu et al., 1998). Maar-only volcanic fields are also
506 observed in back arc basins, such as Espenberg in Alaska and the Megata Volcanic Field in
507 Japan, as well as one example in the compressional Qal'eh Hasan Ali in Iran. Several of these
508 fields only contain a small number of vents (4-20; Table 4), unlike many small volume volcanic
509 fields (monogenetic) that contain hundreds of vents. There are, however, Pleistocene (?)
510 examples of volcanic fields in Tanzania near Mt. Hanang that contain > 100 phreatomagmatic
511 vents (Delcamp et al., 2017). These fields have a diversity of tectonic setting, environment
512 (permafrost, equatorial, arid), and spacing and shape of craters. With the exception of the
513 Qal'eh Ali field in Iran (Milton, 1977), all of these other fields occur in extensional settings with a
514 range of climates. This strongly suggests that while the availability of water is significant, the

515 tectonic setting and the subsurface structure are critical to the conditions leading to maar-
516 forming eruptions.

517 **5.0 Evidence for lateral migration from maar crater size and shape**

518 Planform crater growth is a result of excavation and subsidence by subsurface
519 explosions, and collapse of the crater rim (Valentine and White, 2012; White and Ross, 2011).
520 Analog experiments using buried chemical explosives indicate that the diameter of a crater with
521 a laterally fixed blast location does not grow infinitely (Sonder et al., 2015), suggesting that for
522 very large craters, and complicated crater shapes, lateral migration of the explosion locus is
523 necessary and common (Valentine et al., 2015a). The range of expected phreatomagmatic
524 explosion energies has been estimated from the volume of intrusions observed in eroded
525 volcanic centers (Valentine et al., 2014) and the volume of individual beds in tephra rings
526 (Graettinger and Valentine, 2017). Based on these energies and the observation of asymptotic
527 growth of experimental craters (Sonder et al., 2015) the largest diameter of a single
528 phreatomagmatic explosion in optimal conditions at the largest estimated natural energy (10^{13} J)
529 would be 350 m in diameter. Experimental craters were observed to grow by ~60% in
530 experimental settings with repeated optimal explosions and associated collapse. An ideal crater
531 produced by tens of explosions without lateral migration could likely reach 560 m in diameter.
532 Assuming this value is conservative, attempting to account for crater growth by post-eruption
533 collapse, a crater of 700 m diameter falls in the 35th percentile of the MaarVLS database.
534 Energy transfer in phreatomagmatic explosions is inefficient (Wohletz, 1986; Büttner and
535 Zimanowski, 1998), meaning that these values are more likely to overestimate crater size from
536 an eruption without lateral migration. Therefore, large craters, even with circular morphologies,
537 require lateral vent migration.

538 Field studies have identified evidence of lateral explosion migration in tephra rings
539 surrounding maar craters and exhumed diatreme structures (Ort and Carrasco-Núñez, 2009;

540 van Otterloo et al., 2013; Jordan et al., 2013; López-Rojas and Carrasco-Núñez, 2015;
541 Valentine et al., 2015b). There are numerous influences on lateral migration of vents in growing
542 maars such as the dimensions and geometry of the intrusions feeding the eruption, magma flux
543 along that intrusion, the presence of pre-existing joints or faults, the distribution of water in the
544 subsurface before and during the eruption, and other heterogeneities in the host rock.

545 Volcanic constructs in small volcanic fields frequently show an alignment with regional
546 stress regimes and the orientation of feeder dikes (LeCorvec et al., 2013). The MaarVLS
547 database demonstrates that a majority of maar craters are not ellipses that form along a linear
548 feeder system. In other words the shapes reflect lateral migration in at least two directions and
549 not simply along a single trend (Fig. 1e,f and Fig. 6d). Field observations of a maar-diatreme
550 feeder system in Hopi Buttes Volcanic Field, USA revealed substantial geometric complexity of
551 intrusions, including abundant sills that would make it difficult to produce simple elliptical craters
552 (Muirhead et al., 2016). There are examples of maar craters that represent the simple scenario
553 of eruption locations occurring along a tabular feeder dike, such as crater chains (Fig. 6), but
554 they only represent a portion of the global maar population.

555 Several stratigraphic studies of phreatomagmatic eruptive centers have been used to
556 reconstruct the relative timing and position of explosive vents within a maar to reveal that the
557 migration of explosion locations did not progress along a simple line. Jordan et al. (2013)
558 reconstructed a triangular distribution of vent positions that were occupied at multiple times
559 during the eruption of Purrumbete maar in Australia. Fierstein and Hildreth (2017) demonstrated
560 that the vent locations at Ubehebe Craters migrated in a zigzagging pattern that ultimately
561 produced two intersecting linear trends of craters (Fig. 6). Historic observations of Ukinrek maar,
562 and stratigraphic studies of multiple maars reflect that simultaneous eruptions of multiple vents
563 can further contribute to crater morphology (Self et al., 1980; Jordan et al., 2013; Amin and
564 Valentine, 2017). These studies highlight that maar crater shapes record important elements of
565 the eruption evolution, and that the subsurface process controlling explosion locations are

566 complex. Additional stratigraphic studies and the integration of structural, hydrological, and
567 morphometric data may be useful in determining the typical spacing distance for migrating
568 explosion locations.

569 These morphological observations, in addition to a growing literature on field
570 observations of diatreme and tephra ring structures, including the documentation of magmatic
571 deposits at various times during eruptions, suggest that the production of explosions is not
572 solely limited by water availability rather the geometry of the plumbing system, magmatic flux,
573 and the hydrological properties of the evolving diatreme. Further, the complex shapes of maar
574 craters suggests that growing diatremes exert significant local control on the location of
575 subsequent explosions resulting in large and compound crater shapes at the surface.

576

577 **6.0 Conclusions**

578 MaarVLS is the most comprehensive survey of planform maar morphometry to date and
579 is a useful tool to investigate global trends in maar formation, highlighting the universal traits
580 and unique subsets of these volcanoes. A typical maar crater is not circular, nor a simple
581 ellipse, displaying elongation and large-scale deviations in the curvature of the crater rim with
582 most crater sizes between 600 and 1000 m. Volcanic fields containing maars have a range of
583 crater sizes and shapes where the largest maar crater is commonly less than twice of the size of
584 the smallest maar. Magma composition and occurrence of multiple co-located eruptions through
585 time do not seem to produce diagnostic crater sizes or shapes.

586 The MaarVLS database highlights the importance of lateral growth of craters in more
587 than one direction supporting field-based observations that lateral explosion location is common
588 and fundamental to the evolution of maar-forming eruptions. Additional work to relate shape with
589 host rock properties, regional faults and local hydrology is planned to further isolate the
590 influences on this lateral crater growth. Exceptional populations of large size craters, maar-
591 dominated volcanic fields, and crater chains warrant further study as they have the potential to

592 provide unique insight into the role of regional structures, ground ice, lateral migration, and co-
593 located eruptions on the role of maar formation. Future comparison of this morphometric
594 database with similar datasets for other negative landforms on Earth and Mars should lead to
595 the remote identification of these volcanic features on both planetary surfaces.

596

597 **7.0 Acknowledgments**

598 The MaarVLS database version 1 is available on Vhub (<https://vhub.org/resources/4365>).
599 Additions to this database are requested and updates will be posted periodically. This work was
600 funded in part by the University at Buffalo 3E fund. ASTER and ASTER GDEM is a product of
601 METI and NASA. EarthPoint topo uses data from the Bureau of Land Management and USGS.
602 Esteven Tiñeo Mateo, Yingchen Li, Courtney Tabor and Keith Bennet are thanked for their
603 contribution to crater digitization. T. Gregg and G. Valentine are thanked for the many
604 conversations that led to the production of this database. Thanks to M. Brenna and B. Van Wyk
605 de Vries for their comments on an earlier version of the manuscript. A. Delcamp and an
606 anonymous reviewer are thanked for their suggestions.

607 **8.0 References**

- 608 Amin, J. and Valentine, G.A., 2017. Compound maar crater and co-eruptive scoria cone in the
609 Lunar Crater Volcanic Field (Nevada, USA). *Journal of Volcanology and Geothermal*
610 *Research*, 339: 41-51.10.1016/j.jvolgeores.2017.05.002
- 611 Auer, A., Martin, U. and Nemeth, K., 2007. The Fekete-hegy (Balaton Highland Hungary) "soft-
612 substrate" and "hard-substrate" maar volcanoes in an aligned volcanic complex -
613 Implications for vent geometry, subsurface stratigraphy and the palaeoenvironmental
614 setting *Journal of Volcanology and Geothermal Research*, 159: 225-
615 245.10.1016/j.jvolgeores.2006.06.008
- 616 Avellan, D.R., Macias, J.L., Pardo, N., Scolamacchia, T. and Rodriguez, D., 2012. Stratigraphy,
617 geomorphology, geochemistry and hazard implications of the Nejapa Volcanic Field,
618 western Managua, Nicaragua. *Journal of Volcanology and Geothermal Research*, 213-
619 214: 51-71.doi:10.1016/j.jvolgeores.2011.11.002
- 620 Beget, J.E., Hopkins, D.M. and Charron, S.D., 1996. The Largest known maars on Earth,
621 Seward Peninsula, Northwest Alaska. *Arctic*, 49(1): 62-69
- 622 Bemis KG, Ferencz M (2017) Morphometric analysis of scoria cones: the potential for inferring
623 process from shape. In: Nemeth K, Carrasco Nunez G, Gomez A, Smith IEM (eds)
624 Monogenetic Volcanisms. Geological Society, London, pp 61-100

625 Blaikie, T.N., Ailleres, L., Cas, R.A.F. and Betts, P.G., 2012. Three-dimensional potential field
626 modelling of a multi-vent maar-diatreme -The Lake Coragulac maar, Newer Volcanics
627 Province, south-eastern Australia *Journal of Volcanology and Geothermal Research*,
628 235-236: 70-83.10.1016/j.jvolgeores.2012.05.002

629 Boyce, J., 2013. The Newer volcanic Province of southeastern Australia: a new classification
630 scheme and distribution map for eruption centres. *Australian Journal of Earth Science*,
631 60: 449-462.10.1080/08120099.2013.806954

632 Büttner, R. and Zimanowski, B., 1998. Physics of thermohydraulic explosions. *Physical Review*
633 57: 5726-5730

634 Carn, S., 2000. The Lamongan volcanic field, East Java, Indonesia: physical volcanology,
635 historic activity and hazards. *Journal of Volcanology and Geothermal Research*, 95: 81-
636 108

637 Cas, R.A.F. and Wright, J.V., 1987. *Volcanic Successions*. Allen & Unwin, London, 487 pp.

638 Chako Tchambe, B., Ohba, T., Kereszturi, G., Nemeth, K., Aka, F.T., Youmen, D., Issa,
639 Miyabuchi, Y., Ooki, S., Tanyileke, G. and Hell, J.V., 2015. Towards the reconstruction
640 of the shallow plumbing system of the Barombi Mbo Maar (Cameroon) Implications for
641 diatreme growth processes of a polygenetic maar volcano. *Journal of Volcanology and*
642 *Geothermal Research*, 301: 293-313.10.1016/j.jvolgeores.2015.06.004

643 Chamberlin, R.M., Carther, S.M., Anderson, O.J. and Jones, G.E., 1994. Reconnaissance
644 Geologic Map of the Quemado 30x60 minute quadrangle Catron County, New Mexico.
645 New Mexico Bureau of Mines and Mineral Resources Open File Report, 406: 1-29

646 Delcamp, A., Mattsson, H., Gurioli, L., Bircher, C., Sakoma, E., Belkus, H., Kervyn, M., 2017.
647 Towards an understanding of the North Tanzanian maar crater formation from a cross-
648 disciplinary perspective. *IAVCEI Scientific Assembly Abstracts 2017*, number 328: 254.

649 Delpit, S., Ross, P.-S. and Hearn, B.C., 2014. Deep bedded ultramafic diatremes in Missouri
650 River Breaks volcanic field, Montana, USA: more than 1 km of syn-eruptive subsidence.
651 *Bulletin of Volcanology*.10.1007/s00445-014-0832-8

652 Eakins, B.W. and Sharman, G.F. 2012 Hypsographic curve of Earth's surface from ETOPO1,
653 NOAA National Geophysical Data Center, Boulder, CO.

654 Fierstein, J. and Hildreth, W., 2017. Eruptive history of the Ubehebe Crater cluster, Death
655 Valley, California. *Journal of Volcanology and Geothermal Research*, 335: 128-
656 146.10.1016/j.jvolgeores.2017.02.010

657 Gasparon, M., Innocenti, F., Manetti, P., Peccerillo, A. and Tsegaye, A., 1993. Genesis of the
658 Pliocene to Recent bimodal mafic-felsic volcanism of the Debre Zeyt area, central
659 Ethiopia: volcanological and geochemical constraints. *Journal of African Earth Sciences*,
660 17(2): 145-165

661 Geshi, N., Németh, K. and Oikawa, T., 2011. Growth of phreatomagmatic explosion craters: A
662 model inferred from Suoana crater in Miyakejima Volcano, Japan. *Journal of*
663 *Volcanology and Geothermal Research*, 201: 30-38.10.1016/j.jvolgeores.2010.11.012

664 GlobalVolcanismProgram, 2016. *Volcanoes of the World*. Smithsonian Institution, Washington
665 DC.

666 Graettinger AH, Valentine GA, 2017. Evidence for the relative depths and energies of
667 phreatomagmatic explosions recorded in tephra rings. *Bulletin of Volcanology*, 79:88,
668 doi: 10.1007/s00445-017-1177-x

669 Graettinger, A.H., 2016. MaarVLS: A Database of Maar Caters on Earth to Enable Investigation
670 of Maars on Mars, Lunar and Planetary Science Conference. Lunar and Planetary
671 Institute, Woodlands, Houston, TX.

672 Graettinger, A.H., Valentine, G.A. and Sonder, I., 2015. Circum-crater variability of deposits
673 from discrete, laterally and vertically migrating volcanic explosions: experimental
674 evidence and field implications. *Journal of Volcanology and Geothermal Research*, 308:
675 61-69.doi:10.1016/j.jvolgeores.2015.10.019

676 Graettinger, A.H., Valentine, G.A. and Sonder, I., 2016. Recycling in debris-filled volcanic vents.
677 *Geology*, 44: 811-814.doi:10.1130/G38081.1

678 Gutmann, J.T., 2002. Strombolian and effusive activity as precursors to phreatomagmatism:
679 eruptive sequence at maars of the Pinacate volcanic field, Sonora, Mexico. *Journal of*
680 *Volcanology and Geothermal Research*, 113: 354-356

681 Isaia, R., Vitale, S., Di Giuseppe, M.G., Iannuzzi, E., Tramparulo, F.D.A. and Troiano, A., 2015.
682 Stratigraphy, structure, and volcano-tectonic evolution of Solfatara maar-diatreme
683 (Campi Flegrei, Italy). *GSA Bulletin*.10.1130/B31183.1

684 Jordan, S.C., Cas, R.A.F. and Hayman, P.C., 2013. The origin of a large (>3 km) maar volcano
685 by coalescence of multiple shallow craters: Lake Purrumbete maar, southeastern
686 Australia *Journal of Volcanology and Geothermal Research*, 254: 5-
687 22.10.1016/j.jvolgeores.2012.12.019

688 Kampunzu, A.B., Bonhomme, M.G., Kanika, M., 1998. Geochronology of volcanic rocks and
689 evolution of the Cenozoic Western Branch of the East African Rift System. *Journal of*
690 *African Earth Sciences*, 26: 441-461.

691 Kereszturi, G., Jordan, G., Nemeth, K. and Doniz-Paez, F.J., 2012. Syn-eruptive morphometric
692 variability of monogenetic scoria cones. *Bulletin of Volcanology*, 74: 2171-2185.DOI
693 10.1007/s00445-012-0658-1

694 Kervyn, M., Ernst, G.G.J., Carracedo, J.C. and Jacobs, P., 2012. Geomorphometric variability of
695 “monogenetic” volcanic cones: Evidence from Mauna Kea, Lanzarote and experimental
696 cones. *Geomorphology*, 136: 59-75.10.1016/j.geomorph.2011.04.009

697 Ku, Y.-P., Chen, C.-H., Song, S.-R., Iizuka, Y. and Shen, J.J.-S., 2009. A 2 Ma record of
698 explosive volcanism in southwestern Luzon: Implications for the timing of subducted slab
699 steepening. *Geochemistry, Geophysics, Geosystems*, 6(6):
700 Q06017.10.1029/2009GC002486.

701 Kurszlaukis, S., Mahotkin, I., Rotman, A.Y., Kolesnikov, G.V. and Makovchuk, I.V., 2009. Syn-
702 and post-eruptive volcanic processes in the Yubileynaya kimberlite pipe, Yakutia, Russia,
703 and implications for the emplacement of South African-style kimberlite pipes. *Lithos*,
704 112S: 579-591.doi:10.1016/j.lithos.2009.05.016

705 Le Corvec, N., Spörl, K.B., Rowland, J.V. and Lindsay, J.M., 2013. Spatial distribution and
706 alignments of volcanic centers: Clues to the formation of monogenetic volcanic fields.
707 *Earth-Science Reviews*, 124: 96-114.10.1016/j.earscirev.2013.05.005

708 Leat, P.T., Thompson, R.N., Dickin, A.P., Morrison, M.A. and Hendry, G.L., 1989. Quaternary
709 Volcanism in Northwestern Colorado: Implications for the roles of the asthenosphere and
710 lithosphere in the genesis of continental basalts. *Journal of Volcanology and Geothermal*
711 *Research*, 37: 291-310

712 Lefebvre, N.S., White, J.D.L. and Kjarsgaard, B.A., 2013. Unbedded diatreme deposits reveal
713 maar-diatreme forming eruptive processes: Standing Rocks West, Hopi Buttes, Navajo
714 Nation, USA. *Bulletin of Volcanology*, 75: 739.10.1007/s00445-013-0739-9

715 López-Rojas, M. and Carrasco-Núñez, G., 2015. Depositional facies and migration of the
716 eruptive loci for Atexcac axalapazco (central Mexico): implications for the morphology of
717 the crater. *Revista Mexicana de Ciencias Geológicas*

718 Macorps, E., Graettinger, A.H., Valentine, G.A., Sonder, I., Ross, P.-S. and White, J.D.L., 2016.
719 The effects of the host-substrate properties on maar-diatreme volcanoes. *Bulletin of*
720 *Volcanology*, 78(26).10.1007/s00445-016-1013-8

721 Martín-Serrano, A., Vegas, J., García-Cortés, A., Galán, L., Gallardo-Millán, J.L., Martín-
722 Alfageme, S., Rubio, F.M., Ibarra, P.I., Granda, A., Pérez-González, A. and García-
723 Lobón, J.L., 2009. Morphotectonic setting of maar lakes in the Campo de Calatrava
724 Volcanic Field (Central Spain, SW Europe). *Sedimentary Geology*, 222: 52-
725 63.doi:10.1016/j.sedgeo.2009.07.005

726 Mattsson, H.B. and Tripoli, B.A., 2011. Depositional characteristics and volcanic landforms in
727 the Lake Natron-Engaruka monogenetic field, northern Tanzania. *Journal of Volcanology*
728 and *Geothermal Research*, 203: 23-34.10.1016/j.jvolgeores.2011.04.010

729 Milton, D.J., 1977. Qal'eh Hasan Ali Maars, Central Iran. *Bulletin of Volcanology*, 40(3): 201-208

730 Muirhead, J.D., Van Eaton, A.R., Re, G., White, J.D.L. and Ort, M., 2016. Monogenetic
731 volcanoes fed by interconnected dikes and sills in the Hopi Buttes volcanic field, Navajo
732 Nation, USA. *Bulletin of Volcanology*, 78(11).DOI 10.1007/s00445-016-1005-8

733 Murray, J.B. and Guest, J.E., 1970. Circularities of craters and related structures on Earth and
734 Moon. *Modern Geology*, 1: 149-159

735 Nemeth, K. and Kereszturi, G., 2015. Monogenetic volcanism: personal views and discussion.
736 *International Journal of Earth Sciences*, 104: 2131-2146.DOI 10.1007/s00531-015-1243-
737 6

738 Nemeth, K., Martin, U. and Harangi, S., 2001. Miocene phreatomagmatic volcanism at Tihany
739 (Pannonian Basin, Hungary). *Journal of Volcanology and Geothermal Research*, 111:
740 111-135

741 Ort, M.H. and Carrasco-Núñez, G., 2009. Lateral vent migration during phreatomagmatic and
742 magmatic eruptions at Tecuítlapa Maar, east-central Mexico. *Journal of Volcanology and*
743 *Geothermal Research*, 181: 67-77.10.1016/j.jvolgeores.2009.01.003

744 Palladino, D.M., Valentine, G.A., Sottili, G. and Taddeucci, J., 2015. Maars to calderas: end-
745 members on a spectrum of explosive volcanic depressions. *Frontiers in Earth Science*,
746 3.10.3389/feart.2015.00036

747 Pirrung, M., Buchel, G., Lorenz, V. and Treutler, H.-C., 2008. Post-eruptive development of the
748 Ukinrek East Maar since its eruption in 1977 A.D. in the periglacial area of south-west
749 Alaska. *Sedimentology*, 55: 305-334.10.1111/j.1365-3091.2007.00900.x

750 Ross, P.-S., Delpit, S., Haller, M.J., Németh, K. and Corbella, H., 2011. Influence of the
751 substrate on maar-diatreme volcanoes- An example of a mixed setting from the Pali Aike
752 volcanic field, Argentina. *Journal of Volcanology and Geothermal Research*, 201: 253-
753 271.10.1016/j.jvolgeores.2010.07.018

754 Self, S., Kienle, J. and Huot, J.-P., 1980. Ukinrek Maars, Alaska, II. Deposits and formations of
755 the 1977 craters. *Journal of Volcanology and Geothermal Research*, 7: 39-65

756 Sonder, I., Graettinger, A.H. and Valentine, G.A., 2015. Scaling multiblast craters: general
757 approach and application to volcanic craters. *Journal of Geophysical Research*, 120:
758 6141-6158.10.1002/2015JB012018

759 Sottili, G., Taddeucci, J., Palladino, D.M., Gaeta, M., Scarlato, P. and Ventura, G., 2009. Sub-
760 surface dynamics and eruptive styles of maars in the Colli Albani Volcanic District,
761 Central Italy. *Journal of Volcanology and Geothermal Research*, 180: 189-
762 202.10.1016/j.jvolgeores.2008.07.022

763 Valentine, G.A., Graettinger, A.H., Macorps, E., Ross, P.-S., White, J.D.L., Dohring, E. and
764 Sonder, I., 2015a. Experiments with vertically and laterally migrating subsurface
765 explosions with applications to the geology of phreatomagmatic and hydrothermal
766 explosion craters and diatremes. *Bulletin of Volcanology*, 77: 15.10.1007/s00445-015-
767 0901-7

768 Valentine, G.A., Graettinger, A.H. and Sonder, I., 2014. Explosion depths for phreatomagmatic
769 eruptions. *Geophysical Research Letters*, 41.10.1002/2014GL060096

770 Valentine, G.A., Sottili, G., Palladino, D.M. and Taddeucci, J., 2015b. Tephra ring interpretation
771 in light of evolving maar-diatreme concepts: Stracciaccappa maar (central Italy). *Journal*
772 *of Volcanology and Geothermal Research*, 308: 19-
773 29.doi:10.1016/j.jvolgeores.2015.10.010

774 Valentine, G.A. and White, J.D.L., 2012. Revised conceptual model for maar-diatremes:
775 Subsurface processes, energetics, and eruptive products. *Geology*, 40(12): 1111-
776 1114.10.1130/G33411.1

- 777 van Otterloo, J., Cas, R.A.F. and Sheard, M.J., 2013. Eruption processes and deposit
778 characteristics at the monogenetic Mt. Gambier Volcanic Complex, SE Australia:
779 implications for alternating magmatic and phreatomagmatic activity. *Bulletin of*
780 *Volcanology*, 75: 737.10.1007/s00445-013-0737-y
- 781 White, J.D.L. and Ross, P.S., 2011. Maar-diatreme volcanoes: A review. *Journal of Volcanology*
782 *and Geothermal Research*, 201: 1-29.doi:10.1016/j.jvolgeores.2011.01.010
- 783 Wohletz, K.H., 1986. Explosive magma-water interactions: Thermodynamics, explosions
784 mechanisms, and field studies. *Bulletin of Volcanology*, 48: 245-264
- 785 Wood, C.A. and Kienle, J., 1990. *Volcanoes of North America: United States and Canada.*
786 Cambridge Univ. Press, Cambridge
- 787 Zolitschka, B., Negendank, J.F.W. and Lottermoser, B.G., 1995. Sedimentological proof and
788 dating of the Early Holocene volcanic eruption of Ulmener Maar (Vulkaneifel, Germany).
789 *Geol Rundsch*, 84: 213-219